Chinese Journal of Catalysis 40 (2019) 673–680

available at www.sciencedirect.com

ScienceDirect

journal homepage: www.elsevier.com/locate/chnjc

Article (Special Issue on Environmental and Energy Catalysis for Sustainable Development)

Exploring a broadened operating pH range for norfloxacin removal via simulated solar-light-mediated Bi_2WO_6 process

Meijuan Chen [a,b], Yu Huang [b,*], Wei Chu [c]

[a] School of Human Settlements and Civil Engineering, Xi'an Jiaotong University, Xi'an 710049, Shaanxi, China

[b] State Key Laboratory of Loess and Quaternary Geology (SKLLQG), Key Laboratory of Aerosol Chemistry & Physics, Institute of Earth Environment, Chinese Academy of Sciences, Xi'an 710061, Shaanxi, China

[c] Department of Civil and Environmental Engineering, The Hong Kong Polytechnic University, Hung Hom, Hong Kong, China

ARTICLE INFO

Article history:
Received 13 November 2018
Accepted 13 December 2018
Published 5 May 2019

Keywords:
Bismuth tungstate
Broadened operating pH
Norfloxacin
Photocatalysis
Water

ABSTRACT

Semiconductor photocatalysis can be operated over a narrow pH range for wastewater treatment. In this study, a simulated solar-light-mediated bismuth tungstate (SSL/Bi_2WO_6) process is found to be effective for norfloxacin degradation over a narrow pH range. To broaden the operating pH range of the SSL/Bi_2WO_6 process, an NH_4^+ buffer system and an Fe^{3+} salt were introduced under extremely basic and acidic pH conditions, respectively. The NH_4^+ buffer system continuously supplied hydroxyl ions to generate ·OH radicals and prevented acidification of the solution, resulting in improved norfloxacin removal and mineralization removal under alkaline conditions. In contrast, the Fe^{3+} salt offered an additional homogeneous photo-sensitization pathway. The former treatment assisted in norfloxacin decay and the latter increased the collision frequency between the photo-generated hole and hydroxyl ions. Moreover, the effect of parameters such as pH and Fe^{3+} dosage was optimized.

1. Introduction

Norfloxacin is a second generation synthetic fluoroquinolone antibiotic that has been widely detected in aqueous environments. In Chesapeake Bay, the largest estuary in the United States, the highest aqueous phase concentration of norfloxacin was recorded at 94.1 ng/L [1]. In China, it has been reported that norfloxacin is the most frequently detected antibiotic in coastal waters with a maximum concentration of 1990 ng/L [2]. Furthermore, in an artificial drinking water reservoir in the Yangtze River delta of East China, norfloxacin was detected at a frequency of 97.85%. With the deliberate release of antibiotics into the aqueous environment and lack of effective treatments for antibiotic-contaminated wastewater, antibiotic pollution continues to pose a serious environmental threat to aquatic and terrestrial ecosystems [3]. Therefore, the removal of norfloxacin from aquatic environments is becoming an important issue [4,5].

Different technologies are available for the remediation of norfloxacin, including biological degradation, adsorption, and AOPs, to minimize its damage in aquatic environment [6–8]. Among the emerging treatment approaches, AOPs are consid-

* Corresponding author. Tel/Fax: +86-29-62336261; E-mail: huangyu@ieecas.cn

This work was supported by the National Science Foundation of China (41877481, 41503102), the open project of the State Key Laboratory of Loess and Quaternary Geology, Institute of Earth Environment, Chinese Academy of Science (SKLLQG1729), the China Postdoctoral Science Foundation (2018M643669), the Fundamental Research Funds for the Central Universities (2018249), and the "Hundred Talent Program" of the Chinese Academy of Sciences.
DOI: S1872-2067(19)63285-7 | http://www.sciencedirect.com/science/journal/18722067 | Chin. J. Catal., Vol. 40, No. 5, May 2019

ered to be effective and are currently gaining significant attention in the water treatment industry [9–13]. The pH is considered to be an important factor for photocatalytic performance, as demonstrated by many previous studies [14,15]. Generally, the optimum pH for semiconductor photocatalysts are confined within a narrow range [14,16]. For example, the optimum pH of ZnO photocatalysts was shown to be 11 for the degradation of amoxicillin, ampicillin, and cloxacillin in aqueous solution [17]. The optimum working pH of TiO_2 was reported to be 9.0 for chlorinated aniline degradation [18]. In addition to TiO_2, Bi-based semiconductors have been proven effective for organic pollutant removal [19–22]. Fu et al. [23] showed that B-doped Bi_2WO_6 exhibited the highest degradation efficiency toward RhB removal at a pH of approximately 7.0. Outside of this narrow pH range, the catalytic performance significantly decreased. To increase the decay rate of various pollutants, the initial pH of wastewater was adjusted to an optimum level by addition of acid or base [24,25]. However, Hu et al. [26] reported that the pH decreased during photocatalytic reaction, falling outside of the optimal range, slowing pollutant decay.

Previously, we demonstrated that the pH cannot be maintained throughout the SSL/Bi_2WO_6 process due to the formation of small molecule organic acids and carbon dioxide during ciprofloxacin degradation. The pH continuously decreased during the reaction and eventually the solution pH dropped to 3.0, departing drastically from the optimal pH and was accompanied by the retardation of CIP decay [27]. Rao et al. [28] reported a WO_3 photocatalytic system for monuron degradation, achieving the best performance at pH = 6.0. Furthermore, during the developed process, the monuron molecule was transformed to a simple aliphatic acid, resulting in decreased solution pH and retardation of total organic carbon (TOC) removal. In the UV/TiO_2 degradation simazine process, the best degradation efficiency was obtained at an initial pH of approximately 9, and the photocatalytic reaction was retarded under strongly acidic and extreme basic conditions [29]. Meanwhile, the stable cyanuric acid was formed upon the oxidative decomposition of simazine, resulting in acidification of the aqueous solution. Bi_2O_3/$Bi_2O_2CO_3$ was proven to be effective for catalyzing ciprofloxacin decay at neutral pH, but the pH of the final aqueous solution became acidic [15]. Despite the solution pH decrease and inhibited efficiency for the photocatalytic degradation of organic pollutants, few studies have investigated possible solutions to this problem to maintain high catalytic performance at different solution pH values.

Bismuth tungstate (Bi_2WO_6) is the most studied visible light-driven photocatalyst due to its wide spectrum light response and lack of secondary contamination after utilization [30,31]. Moreover, Bi_2WO_6 is composed of perovskite-like $[WO_4]^{2-}$ layers sandwiched between $[Bi_2O_2]^{2+}$ layers. This structure is beneficial for separating photoexcited electron-hole pairs and forming internal electric fields between slabs, which enhances photocatalytic performance [32]. In addition, Bi_2WO_6 is stable in aqueous solution without dissolving or element leaching [27,33].

In this study, innovative approaches were proposed to expand the operating pH range for simulated solar light-mediated Bi_2WO_6 photocatalysis (SSL/Bi_2WO_6). Norfloxacin was selected as the target antibiotic compound. The performance for norfloxacin degradation at different pH values were studied in the proposed SSL/Bi_2WO_6 process. To broaden the operating pH range, efforts were undertaken to achieve high removal efficiency under extremely basic and acidic pH conditions. At an extremely basic pH, a buffer system was developed using an NH_4^+ salt and at extremely acidic pH, the SSL/Bi_2WO_6 process was improved by adding ferric salts.

2. Experimental

2.1. Chemical and reagents

All chemicals were of analytical reagent grade and used as-received without further purification. Norfloxacin ($C_{16}H_{18}FN_3O_3$) was purchased from Wako Pure Chemical Industries, Ltd. and used as the target molecule for degradation. Bi_2WO_6 was synthesized using tungsten acid (H_2WO_4), citric bismuth ($C_6H_5BiO_7$), and ammonia ($NH_3{\cdot}H_2O$) as precursors. The synthesis of bismuth tungstate was reported in detail in the literature [33,34], where the characterizations of Bi_2WO_6 via X-ray diffraction (XRD), scanning electron microscopy (SEM), transmission electron microscopy (TEM), N_2 adsorption-desorption, ultraviolet-visible diffuse reflectance spectroscopy (UV-Vis DRS) have been well documented. The phase of the obtained product was evaluated by XRD and all diffraction peaks were indexed to pure orthorhombic Bi_2WO_6 with JCPDF No. 39-256. The point of zero charge was tested using a mass titration method [35]. Other chemicals used in this study including $Mg(NO_3)_2$, $Ca(NO_3)_2$, $Fe(NO_3)_3{\cdot}9H_2O$, NaOH, HCl, and H_3PO_4 were obtained from Sigma Aldrich Inc. The mobile phase solvent for HPLC analysis (acetonitrile) was purchased from Tedia Company (USA). Distilled-deionized water with a resistivity of 18.2 MΩ of was used for preparing the mobile phase and stock solutions and was generated using a Barnstead NANOpure water treatment system (Thermo Fisher Scientific Inc., USA).

2.2. Experimental procedures

Norfloxacin degradation was conducted in a simulated solar light photochemical reactor (Beijing Changtuo Company with a Xenon lamp of 300 W). Prior to the reaction, a predetermined amount of Bi_2WO_6 was added to 100 mL of the norfloxacin solution in a 200-mL quartz beaker/cylinder and stirred under darkness for 30 min to reach adsorption equilibrium (pre-adsorption step). After reaching equilibrium, degradation was started by turning on the pre-heated light source. At preset intervals, 1 mL aliquots of the sample were withdrawn and filtered using a 0.2-μm PTFE membrane for further analysis. All experiments were performed in duplicate at room temperature (air-conditioned) at 23±1 °C.

2.3. Analytical methods

The amount of norfloxacin remaining in the solution was

quantified using high-performance liquid chromatography (HPLC) system with a Waters 515 pump, Waters 2489 dual λ absorbance detector, and Waters 717 plus autosampler. The norfloxacin in the solution was separated from its related intermediates using a Restek pinnacle II C18 column (5.0 μm, 4.6 × 250 mm) and quantified via adsorption at 280 nm. A mixture of 50% acetonitrile and 50% 0.025 mmol/L orthophosphoric acid was selected as the mobile phase at a flow rate of 0.8 mL/min, and 10 μL samples were injected for analysis. Parts of the experiment were run in triplicate with relative standard deviations never exceeding 10%. The pH was measured using a digital pH meter (HANNA instrument, B417). Unless otherwise specified, the pH was measured from the solution just prior to reaction. The TOC was analyzed using a Shimadzu TOC-5000A analyzer equipped with an ASI-5000A autosampler to determine the mineralization of norfloxacin using this process.

3. Results and discussion

3.1. Degradation performance at different pH values

Norfloxacin degradation was performed at different pH values ranging from 3.0 to 13.0, and the decay curves are shown in Fig. 1. The decay was significantly reduced under extremely acidic (pH = 3.0) and alkaline (pH 13.0) conditions due to the electrostatic repulsion between the norfloxacin molecule and Bi_2WO_6 particle surface, arising from the p*K*a of norfloxacin (pK_{a1} = 6.34, pK_{a2} = 8.75) and the point of zero charge of Bi_2WO_6 (pH = 5.0). Three species of norfloxacin can exist in solution (cationic, zwitterionic, and anionic) and two phases of Bi_2WO_6 (cationic and anionic at a pH of 5.0) with variable pH. Under acidic (pH <5.0) and basic pH conditions (pH >8.75), both norfloxacin and Bi_2WO_6 mostly exist as like charges, preventing attraction between them and inhibiting norfloxacin decay.

On the other hand, a moderate pH range (i.e. pH = 5.0 to 10.8) is favorable for norfloxacin decay, where all tests at moderate pH showed >90% norfloxacin removal in 150 min. However, norfloxacin decay in the moderate pH range still showed certain differences as a function of pH. In particular, the optimal performance was observed at pH = 8.6, showing 93% norfloxacin removal in 60 min. From pH = 5.0 to 8.6, the norfloxacin removal efficiency gradually increased, indicating that higher pH values improved norfloxacin decomposition as long as the Bi_2WO_6 and norfloxacin remained electrostatically attractive. For pH values slightly higher than that of pK_{a2} (i.e. pH at 9.0 and 10.8), inhibition of norfloxacin decay was observed, which can be attributed to the repulsive forces between norfloxacin and Bi_2WO_6 at this pH that restrict interaction between norfloxacin and the Bi_2WO_6 surface. Despite the repulsive force preventing norfloxacin removal, it was interesting that the removal efficiency at pH = 9.0 (repulsive force) was superior to that at pH = 7.5 (attractive force), suggesting the pH itself has a significant effect on norfloxacin decay, and can even be considered more critical than the electrostatic effect in some cases.

3.2. Variations in pH during norfloxacin decay

The pH variations during the pre-adsorption and reaction steps were monitored at three pH values, and the results are shown in Fig. 2. All three runs showed a continuous pH decrease, regardless of initial pH value. During the pre-adsorption stage, the pH quickly dropped from 10.0, 9.3, and 8.1 to 8.6, 7.8, and 7.5, respectively. This significant pH decrease in the pre-adsorption step indicated that hydroxyl ions in the solution were adsorbed (or at least attracted) to the Bi_2WO_6 surface. This was critical for the SSL/Bi_2WO_6 process as it provided a reservoir of precursors for the formation of hydroxyl radicals in the subsequent (reaction) step, where the hydroxyl radical was the dominating active species, as determined by quenching experiments [27]. An OH^- enriched model was proposed to describe this property of Bi_2WO_6 and is shown in Scheme 1, where the hydroxyl ions adhered and concentrated on the Bi_2WO_6 surface and its surroundings. After initiation of the photocatalytic reaction, the pH continuously decreased at a lower rate, suggesting that the hydroxyl ions were gradually consumed in the degradation process, likely due to the formation of low molecular weight organic acids and carbon di-

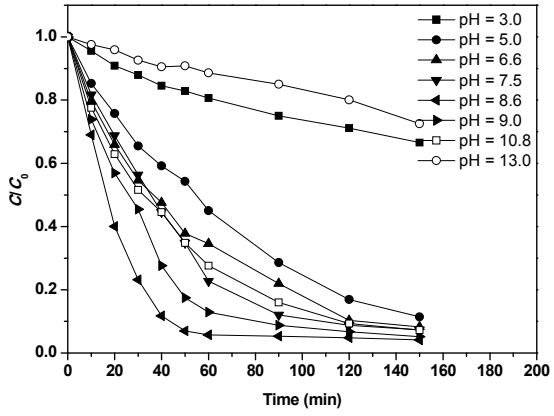

Fig. 1. Effect of pH on the SSL/Bi_2WO_6 process. Experimental conditions: [Norfloxacin]$_0$ = 0.1 mmol/L, [Bi_2WO_6] = 1 g/L.

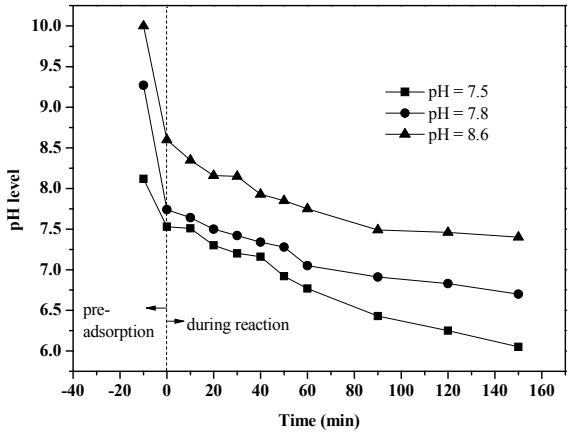

Fig. 2. Variations of pH during the SSL/Bi_2WO_6 reaction. Experimental conditions: [Norfloxacin]$_0$ = 0.1 mmol/L, [Bi_2WO_6] = 1 g/L.

oxide.

Considering the pH decrease during the SSL/Bi_2WO_6 process, it is clear that the norfloxacin decay rate may be gradually hindered if the pH is shifted to an unfavorable range. It is well-known that only the hydroxyl ions close to the Bi_2WO_6 surface can be the source of active hydroxyl radicals due to the limited lifetime of the photo-generated holes [36]. Therefore, the maintenance of higher hydroxyl ion concentrations nearby or on the Bi_2WO_6 surface is critical for improving or maintaining rapid target decomposition.

3.3. The effect of calcium and magnesium salts

To verify the proposed OH^- enriched model, norfloxacin decay in the presence of calcium and magnesium salts was investigated due to their similar chemical properties and large differences hydroxyl ion capture abilities. The K_{sp} (solubility product constant) of $Mg(OH)_2$ and $Ca(OH)_2$ are 1.5×10^{-11} and 0.166, respectively. Thus, it can be deduced that the magnesium ions more effectively deplete hydroxyl ions and generate magnesium hydroxide at lower $[OH^-]$ compared to that of calcium ions. As described in the OH^- enriched model in Scheme 1, the hydroxyl ions were adsorbed onto the Bi_2WO_6 surface to form a thin layer of concentrated OH^-. It is presumed that once the metal salt dosages are properly administered, the hydroxyl ions originally concentrated on the Bi_2WO_6 surface are removed by the magnesium ion, resulting in reduced hydroxyl radical generation. However, this procedure is ineffective when using calcium salts, due to their higher K_{sp} values.

Detailed investigations were performed by varying the $[Ca^{2+}]$ and $[Mg^{2+}]$ from 0 to 40 mmol/L, and the results are shown in Fig. 3. The calcium ions showed no effect on norfloxacin degradation, even when the $[Ca^{2+}]$ was increased to 40 mmol/L. However, magnesium significantly retarded norfloxacin decay and higher $[Mg^{2+}]$ resulted in a slower norfloxacin decay rates. The norfloxacin remaining after 20 min of degradation was 22.9%, 29.0%, 31.9%, 38.3%, and 42.1% at $[Mg^{2+}]$ of 0, 10, 20, 30, and 40 mmol/L, respectively. These experimental results are quite encouraging and support the assumptions presented in Scheme 1, where the concentration of hydroxyl ions surrounding Bi_2WO_6 is sufficient for the production of $Mg(OH)_2$, but not for $Ca(OH)_2$ formation, This also validates the proposed OH^- enriched model in Scheme 1. Therefore the hydroxyl ion concentration in the thin layer surrounding Bi_2WO_6 was calculated to be between 3.87×10^{-4} and 2.03 mol/L in the tests based on the K_{sp} values and concentrations of magnesium and calcium salts (10 and 40 mmol/L, respectively). The calculation method is as follows, i.e. when $[Mg^{2+}]$ = 10 mmol/L, the formation of $Mg(OH)_2$ suggested $[Mg^{2+}]\cdot[OH^-]^2 < 1.5\times10^{-11}$ (Ksp of $Mg(OH)_2$), thus $[OH]^-$ was calculated as greater than 3.87×10^{-4} mol/L; when $[Ca^{2+}]$ = 40 mmol/L, the non-formation of $Ca(OH)_2$ suggested $[Ca^{2+}]\cdot[OH^-]^2 > 0.166$ (Ksp of $Ca(OH)_2$), thus $[OH]^{-}$ was calculated to be less than 2.03 mol/L.

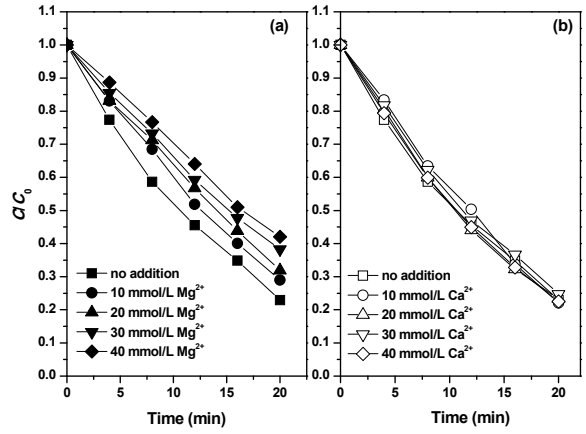

Fig. 3. Effect of Ca^{2+} (a) and Mg^{2+} (b) on the SSL/Bi_2WO_6 process. Experimental conditions: $[Norfloxacin]_0$ = 0.0313 mmol/L, $[Bi_2WO_6]$ = 0.5 g/L.

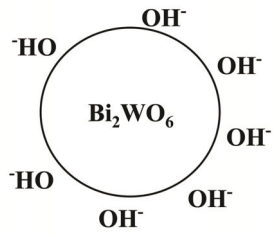

Scheme 1. OH^--enriched Bi_2WO_6 model.

The experiments showed that the pre-adsorption capacity of Bi_2WO_6 for norfloxacin was decreased in the presence of Mg^{2+}, and further decreased with increasing $[Mg^{2+}]$. When $[Mg^{2+}]$ was 0, 10, 20, 30, and 40 mmol/L, the pre-adsorption efficiency of norfloxacin was 7.1%, 6.2%, 4.8%, and 2.7%, respectively. These variations in pre-adsorption efficiency can also be ascribed to the formation of magnesium hydroxides near the Bi_2WO_6 surface, which left fewer adsorption sites available for norfloxacin and blocked the diffusion pathway for norfloxacin to the Bi_2WO_6 surface. However, in the presence of Ca^{2+} ions no pre-adsorption variation was observed because the surface properties of Bi_2WO_6, as shown in the OH^- enriched model, remained largely unchanged, even at a high $[Ca^{2+}]$ of 40 mmol/L. The pre-adsorption variation in the presence of Mg^{2+}, and its insensitivity toward Ca^{2+} further justify the proposed OH^- enrichment model.

3.4. Norfloxacin decay at basic pH

Norfloxacin decay under extremely basic pH conditions was significantly slowed, as shown in Fig. 4. At pH = 13.0, only 22.0% of the norfloxacin was removed after 150 min. Considering that the hydroxyl ion is the source of the active radical ·OH, an ammonium salt (NH_4Cl) was gradually added to the reaction solution to decrease the pH to 9.0 by forming a buffer system, as shown in Fig. 4. The ammonium salt was chosen because it is a natural degradation product of nitrogenous organic matter, and significant sources of enrichment include industrial waste, municipal wastewater treatment plants, and agricultural runoff (including animal wastes and chemical fertilizers) [37]. From Fig. 4, it is clear that after dosing ammonium,

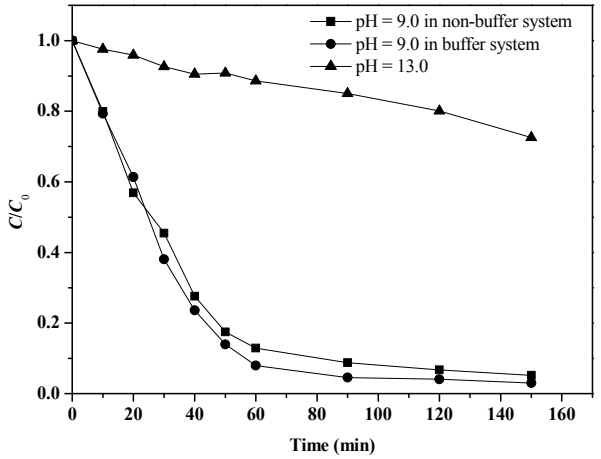

Fig. 4. Norfloxacin decay under extremely basic conditions in different systems. Experimental conditions: $[Norfloxacin]_0$ = 0.1 mmol/L, $[Bi_2WO_6]$ = 1 g/L.

norfloxacin decay efficiency dramatically increased to 97.0% in 60 min. This observation indicates that the pH adjustment by forming a buffer system with simple addition of an NH_4^+ salt under extremely basic condition is a practical method for the SSL/Bi_2WO_6 process.

Furthermore, a comparison experiment was performed using a non-buffered system, where the solution pH was initially set at 13.0, followed by adjustment to 9.0 using HCl. As shown in Fig. 4, norfloxacin decay in the non-buffered system was slightly slower than that of the NH_4Cl buffer system. This is because in the non-buffered system the pH gradually decreased from 9.0 to 8.8 (10 min), 8.3 (20 min), and 7.0 (150 min), which was far from the optimum working pH of 8.6. In contrast, a constant pH was maintained at 9.0 in the buffered system. In addition, TOC removal was investigated, as shown in Fig. 5. Mineralization at pH = 13.0 was negligible, whereas the buffered and non-buffered systems at pH = 9.0 showed 52.0% and 30.0% TOC removal, respectively. Comparing the buffered and non-buffered systems, it was clear that the difference in TOC removal was approximately 22.0%, higher than the difference in norfloxacin removal efficiency (i.e. 3.8% calculated from Fig. 4). This demonstrated that the mineralization of intermediates/byproduct is more efficient in the buffered system.

3.5. Norfloxacin decay at acidic pH

When the aqueous solution is acidic, ferric salts were added to the solution to form the SSL/Fe^{3+}/Bi_2WO_6 process. Fe^{3+} was used because SSL/Fe^{3+} (simulated solar-light-irradiated ferric salt) is efficient at acidic pH for the evaluation of norfloxacin decay. In Fig. 6, the SSL/Fe^{3+} process showed a certain capacity for norfloxacin decay at pH = 4.0. Its mechanism can be rationalized by the oxidative properties of the ferric ions under acidic conditions when irradiated with UV light from the simulated solar light (200–400 nm) [38]. In the acidic solution, Fe^{3+} undergoes spontaneous hydrolysis with water to form a species of $Fe^{III}OH^{2+}$, which is a photosensitive species, and this complex can produce hydroxyl radicals directly via a photo-sensitization reaction:

$$Fe^{III}(OH)^{2+} + h\nu \rightarrow Fe^{2+} + \cdot OH \quad (1)$$

Fig. 6 showed that the removal efficiencies at 20 min in the SSL/Fe^{3+}/Bi_2WO_6, SSL/Fe^{3+}, and SSL/Bi_2WO_6 processes were 75.3%, 44.2%, and 42.4%, respectively. Among these processes, the fastest norfloxacin decay was observed in the SSL/Fe^{3+}/Bi_2WO_6 process. This superior performance at acidic pH can be ascribed to the combination of the advantages of homogeneous SSL/Fe^{3+} and heterogeneous SSL/Bi_2WO_6 processes.

A series of parallel experiments were performed at pH = 7.2 and 9.0 for the above-mentioned three processes and the results are listed in Table 1. The SSL/Fe^{3+} process was largely inert (i.e., no norfloxacin removal was observed) at both pH = 7.2 and 9.0 because the reaction described by Eq. (1) could not proceed at non-acidic pH. In addition, the SSL/Fe^{3+}/Bi_2WO_6 process was slightly superior compared to the SSL/Bi_2WO_6 process at pH = 7.2 (by 5.9%) and 9.0 (by 4.0%) after 20 min of reaction. This improvement can be ascribed to the electron

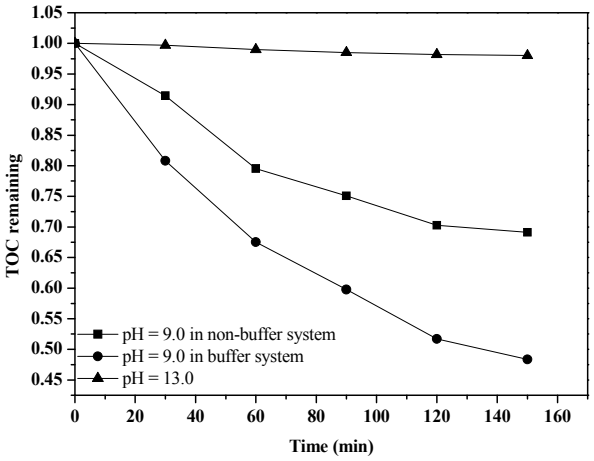

Fig. 5. TOC removal at extremely basic pH conditions in different systems. Experimental conditions: $[Norfloxacin]_0$ = 0.1 mmol/L, $[Bi_2WO_6]$ = 1 g/L.

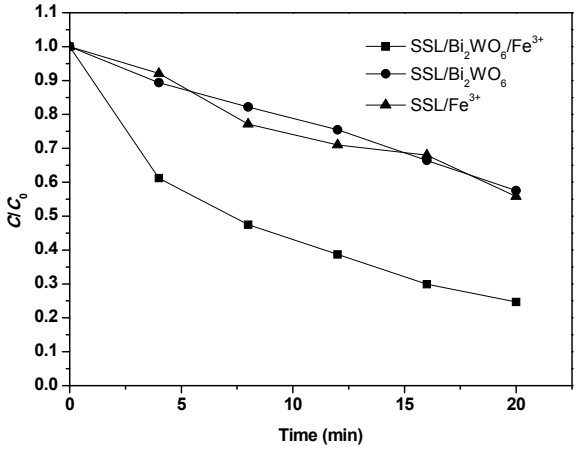

Fig. 6. Norfloxacin decay at an acidic pH of 4 in different processes. Experimental conditions: $[Norfloxacin]_0$ = 0.0313 mmol/L, $[Bi_2WO_6]$ = 0.5 g/L, $[Fe^{3+}]$ = 0.3 mmol/L, pH = 4.0.

Table 1
Norfloxacin decay at acidic, neutral, and basic pH.

System	k, min^{-1}			Removal after 20 min (%)		
	pH = 4.0	pH = 7.2	pH = 9.0	pH = 4.0	pH = 7.2	pH = 9.0
SSL/Fe^{3+}	0.0277	0.0000	0.0000	44.2	0.0	0.0
SSL/Bi_2WO_6	0.0261	0.0679	0.0938	42.4	74.1	85.7
SSL/Fe^{3+}/Bi_2WO_6	fast (non-first order)	0.0777	0.1006	75.3	80	89.7

Experimental conditions: $[Norfloxacin]_0$ = 0.0313 mmol/L, $[Bi_2WO_6]$ = 0.5 g/L, $[Fe^{3+}]$ = 0.3 mmol/L.

transfer carrier role of Fe^{3+}, as shown in Eq. (2), resulting in decreased photogenerated electron-hole combination, which prolonged the lifetime of photo-generated holes and promoted the generation of ·OH radicals [39].

$$Fe^{3+} + e^- \rightarrow Fe^{2+} \quad (2)$$

This observation suggests that Fe^{3+} as an electron transfer carrier also benefitted the SSL/Fe^{3+}/Bi_2WO_6 process under acidic pH conditions.

3.6. Determining the optimum operating pH for the SSL/Fe^{3+}/Bi_2WO_6 process

To determine the optimum pH level for norfloxacin degradation by the SSL/Fe^{3+}/Bi_2WO_6 process, the decay performance at different acidic pH values (i.e. 2.0, 3.0, and 4.0) was investigated and the results are shown in Fig. 7. The SSL/Fe^{3+}/Bi_2WO_6 process at pH = 3.0 showed the most rapid norfloxacin decay, where 82.0%, 86.0%, and 78.3% of the norfloxacin was decomposed at a pH of 2.0, 3.0, and 4.0, respectively, in 20 min. The pH variations during all three runs were negligible and both norfloxacin and Bi_2WO_6 were positively charged with the repulsive force between the two materials preventing norfloxacin decay. Therefore, the difference in performance with pH variation was not a result of the electrostatic effect between norfloxacin and Bi_2WO_6.

It is well-known that Fe^{3+} undergoes spontaneous hydrolysis with water to form four species of Fe(III)-hydroxo complexes, $Fe^{III}OH^{2+}$, $Fe^{III}(OH)_2^+$, $Fe^{III}{}_2(OH)_2^{4+}$, and $Fe^{III}(OH)_3^0$, in an aqueous solution [40]. Moreover, Flynn at el. [41] Reported that the monohydroxy complex $Fe^{III}OH^{2+}$, which is the most photosensitive and photoactive species, was predominant at pH = 3.0. The slowing of norfloxacin decay at pH 4.0 can be attributed to the formation of $Fe^{III}(OH)_3^0$ [42], which results in a decreased $[Fe^{III}OH^{2+}]$ in the solution. On the other hand, the norfloxacin removal performance also decreased when the initial pH decreased to 2.0. This is because the hydrolysis of ferric ions at pH 2.0 was inhibited leading to slower generation of $Fe^{III}OH^{2+}$ [41].

3.7. Effect of $[Fe^{3+}]$ in the SSL/Fe^{3+}/Bi_2WO_6 process

Fig. 8 shows the effect of $[Fe^{3+}]$ on norfloxacin decay in the SSL/Fe^{3+}/Bi_2WO_6 process at the optimum pH of 3.0. After 20 min, the removal efficiency at $[Fe^{3+}]$ of 0.1, 0.2, 0.3, and 0.5 mmol/L was 23.6%, 71.0%, 88.0%, and 86.2%, respectively. As shown in the inset of Fig. 8, $[Fe^{3+}]$ significantly changed the decay rate of norfloxacin, increasing with increased $[Fe^{3+}]$, which plateaued after the critical concentration of 0.3 mmol/L. As described previously, the $Fe^{III}OH^{2+}$ species is essential for norfloxacin decay in the SSL/Fe^{3+}/Bi_2WO_6 process. Higher $[Fe^{3+}]$ provided a larger amount of $Fe^{III}OH^{2+}$ for hydroxyl radical generation. However, if Fe^{3+} is present in excess, too many ·OH radicals will be produced, resulting in the self-reaction of ·OH radicals [43]. Therefore, excess $[Fe^{3+}]$ is not suggested in practical operation.

4. Conclusions

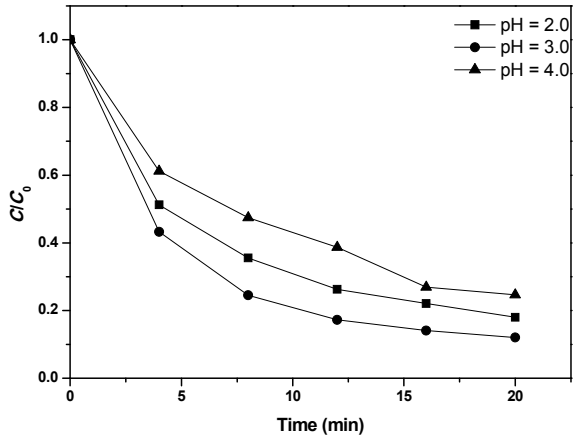

Fig. 7. Norfloxacin decay at different acidic pH values in the SSL/Fe^{3+}/Bi_2WO_6 process. Experimental conditions: $[Norfloxacin]_0$ = 0.0313 mg/L, $[Bi_2WO_6]$ = 0.5 g/L, $[Fe^{3+}]$ =0.3 mmol/L.

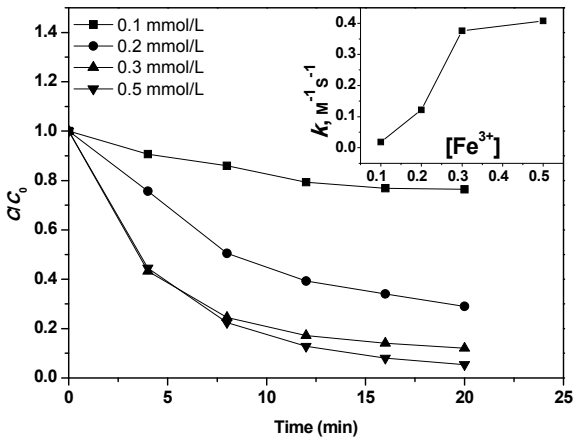

Fig. 8. Norfloxacin decay at different $[Fe^{3+}]$ in the SSL/Fe^{3+}/Bi_2WO_6 process. Experimental conditions: $[Norfloxacin]_0$ = 0.0313 mg/L, $[Bi_2WO_6]$ = 0.5 g/L, at pH =3.0.

In this study, the SSL/Bi_2WO_6 process was used to decompose the antibiotic norfloxacin. The pH significantly influenced the performance in the SSL/Bi_2WO_6 process, which generally exhibited good performance over a narrow pH range. To describing the reaction mechanism of the SSL/Bi_2WO_6 process, an OH^- enriched Bi_2WO_6 model was proposed and verified experimentally by adding Mg^{2+} and Ca^{2+}. Moreover, the hydroxyl ion concentrations in the thin layer surrounding Bi_2WO_6 were determined to range between 3.87×10^{-4} and 2.03 mol/L. Under acidic and alkaline pH conditions, the SSL/Bi_2WO_6 process was significantly inhibited. To broaden the operating pH range of the SSL/Bi_2WO_6 process, different modifications of the original approach were explored. At extremely basic pH, a buffer was successfully introduced into the SSL/Bi_2WO_6 process by simply adding an NH_4^+ salt, which showed excellent performance for both norfloxacin decay and TOC removal. At the extremely acidic pH, the SSL/Bi_2WO_6 process was significantly improved by adding ferric salts (i.e. forming an alternative SSL/Fe^{3+}/Bi_2WO_6 process). The improvement can be ascribed to the homogeneous photo-sensitization mechanism offered by the SSL/Fe^{3+}, whereas the electron transfer carrier role of Fe^{3+} in the SSL/Bi_2WO_6 process was relatively minor. The SSL/Fe^{3+}/Bi_2WO_6 process can be used over a wide acidic pH range (2–4); however, a pH of 3.0 showed slightly better performance. The optimal [Fe^{3+}] for the SSL/Fe^{3+}/Bi_2WO_6 process was 0.3 mmol/L, and the decay rate increased with increasing [Fe^{3+}], then plateaued when ferric ion where in excess.

References

[1] K. He, E. Hain, A. Timm, M. Tarnowski, L. Blaney, *Sci. Total Environ.*, **2019**, 650, 3101–3109.
[2] J. Lu, J. Wu, C. Zhang, Y. Zhang, Y. Lin, Y. Luo, *Sci. Total Environ.*, **2018**, 644, 1469–1476.
[3] D. Li, W. D. Shi, *Chin. J. Catal.*, **2016**, 37, 792–799.
[4] K. Wang, H. Ma, S. Pu, C. Yan, M. Wang, J. Yu, X. Wang, W. Chu, A. Zinchenko, *J. Hazard. Mater.*, **2019**, 362, 160–169.
[5] M. Z. Guo, A. Maury-Ramirez, C. S. Poon, *J. Clean. Prod.*, **2016**, 112, 3583–3588.
[6] S. Q. Liu, Z. Chen, N. Zhang, Z. R. Tang, Y. J. Xu, *J. Phys. Chem. C*, **2013**, 117, 8251–8261.
[7] S. Pu, Y. Hou, H. Chen, D. Deng, Z. Yang, S. Xue, R. Zhu, Z. Diao, W. Chu, *Catalysts*, **2018**, 8, 251/1–251/7.
[8] M. Z. Guo, T.C. Ling, C. S. Poon, *Cem. Concr. Compos.*, **2013**, 36, 101–108.
[9] S. Pu, Y. Hou, C. Yan, H. Ma, H. Huang, Q. Shi, S. Mandal, Z. Diao, W. Chu, *ACS Sustainable Chem. Eng.*, **2018**, 6, 16754–16765.
[10] M. Hui, S. Pu, Y. Hou, R. Zhu, Z. Anatoly, C. Wei, *Chem. Eng. J.*, **2018**, 345, 556–565.
[11] S. Pu, R. Zhu, H. Ma, D. Deng, X. Pei, F. Qi, W. Chu, *Appl. Catal. B*, **2017**, 218, 208–219.
[12] Y. Huang, Y. Gao, Q. Zhang, Y. Zhang, J. J. Cao, W. Ho, S.C. Lee, *J. Hazard. Mater.*, **2018**, 354, 54–62.
[13] Y. Huang, D. Zhu, Q. Zhang, Y. Zhang, J. J. Cao, Z. Shen, W. Ho, S. C. Lee, *Appl. Catal. B*, **2018**, 234, 70–78.
[14] M. Chen, W. Chu, J. Beiyuan, Y. Huang, *Chin. J. Catal.*, **2018**, 39, 701–709.
[15] M. Chen, J. Yao, Y. Huang, H. Gong, W. Chu, *Chem. Eng. J.*, **2018**, 334, 453–461.
[16] Y. Huang, P. Wang, Z. Wang, Y. Rao, J. J. Cao, S. Pu, W. Ho, S. C. Lee, *Appl. Catal. B*, **2019**, 240, 122–131.
[17] E. S. Elmolla, M. Chaudhuri, *J. Hazard. Mater.*, **2010**, 173, 445–449.
[18] W. Chu, W. K. Choy, T. Y. So, *J. Hazard. Mater.*, **2007**, 141, 86–91.
[19] J. Liao, L. Chen, M. Sun, B. Lei, X. Zeng, Y. Sun, F. Dong, *Chin. J. Catal.*, **2018**, 39, 779–789.
[20] Y. Sun, X. Xiao, X. A. Dong, F. Dong, W. Zhang, *Chin. J. Catal.*, **2017**, 38, 217–226.
[21] A. Geng, L. Meng, J. Han, Q. Zhong, M. Li, S. Han, C. Mei, L. Xu, L. Tan, L. Gan, *Cellulose*, **2018**, 25, 4133–4144.
[22] L. Gan, L. J. Xu, K. Qian, Y. D. Wang, F. Y. Jiang, *New Carbon Mater.*, **2018**, 33, 221–228.
[23] Y. Fu, C. Chang, P. Chen, X. Chu, L. Zhu, *J. Hazard. Mater.*, **2013**, 254–255, 185–192.
[24] W. Y. Wang, Y. Ku, *Colloids Surf. A*, **2007**, 302, 261–268.
[25] M. Pelaez, A. A. de la Cruz, K. O'Shea, P. Falaras, D. D. Dionysiou, *Water Res.*, **2011**, 45, 3787–3796.
[26] L. Hu, G. Zhang, M. Liu, Q. Wang, P. Wang, *Chem. Eng. J.*, **2018**, 338,

Graphical Abstract

Chin. J. Catal., 2019, 40: 673–680 doi: S1872-2067(19)63285-7

Exploring a broadened operating pH range for norfloxacin removal via simulated solar-light-mediated Bi_2WO_6 process

Meijuan Chen, Yu Huang *, Wei Chu
Xi'an Jiaotong University; Institute of Earth Environment, Chinese Academy of Sciences; The Hong Kong Polytechnic University

To broaden the operating pH range for Bi_2WO_6 photocatalysis, innovative approaches were designed by creating a buffer system using an NH_4^+ salt under basic pH conditions or introducing a homogeneous SSL/Fe^{3+} photo-sensitization under acidic conditions.

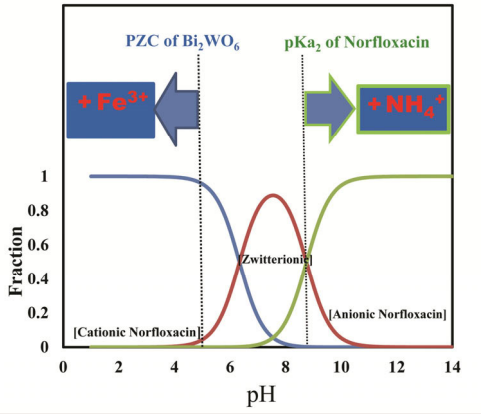

300–310.
[27] M. Chen, W. Chu, *Appl. Catal. B*, **2015**, 168–169, 175–182.
[28] W. Chu, Y. F. Rao, *Chemosphere*, **2012**, 86, 1079–1086.
[29] W. Chu, Y. Rao, W. Y. Hui, *J. Agr. Food Chem.*, **2009**, 57, 6944–6949.
[30] T. Huang, Y. Li, X. Wu, K. Lv, Q. Li, M. Li, D. Du, H. Ye, *Chin. J. Catal.*, **2018**, 39, 718–727.
[31] J. Xu, J. Yue, J. Niu, M. Chen, F. Teng, *Chin. J. Catal.*, **2018**, 39, 1910–1918.
[32] H. Yi, L. Qin, D. Huang, G. Zeng, C. Lai, X. Liu, B. Li, H. Wang, C. Zhou, F. Huang, S. Liu, X. Guo, *Chem. Eng. J.*, **2019**, 358, 480–496.
[33] M. Chen, W. Chu, *Ind. Eng. Chem. Res.*, **2012**, 51, 4887–4893.
[34] Y. Huang, Z. Ai, W. Ho, M. Chen, S. Lee, *J. Phys. Chem. C*, **2010**, 114, 6342–6349.
[35] M. Bellardita, A. Di Paola, B. Megna, L. Palmisano, *Appl. Catal. B*, **2017**, 201, 150–158.
[36] M. A. Fox, M. T. Dulay, *Chem. Rev.*, **1993**, 93, 341–357.
[37] T. Augspurger, A. E. Keller, M. C. Black, W. G. Cope, F. J. Dwyer, *Environ. Toxicol. Chem.*, **2003**, 22, 2569–2575.
[38] H. Měšťánková, G. Mailhot, J. Jirkovský, J. Krýsa, M. Bolte, *Environ. Chem. Lett.*, **2009**, 7, 127–132.
[39] G. R. Bamwenda, T. Uesigi, Y. Abe, K. Sayama, H. Arakawa, *Appl. Catal. A*, **2001**, 205, 117–128.
[40] R. L. Martin, P. J. Hay, L. R. Pratt, *J. Phys. Chem. A*, **1998**, 102, 3565–3573.
[41] C. M. Flynn, *Chem. Rev.*, **1984**, 84, 31–41.
[42] B. Ensing, F. Buda, E. J. Baerends, *J. Phys. Chem. A*, **2003**, 107, 5722–5731.
[43] M. E. Lindsey, M. A. Tarr, *Chemosphere*, **2000**, 41, 409–417.

宽pH条件下运行的太阳光催化钨酸铋降解抗生素诺氟沙星

陈美娟[a,b], 黄　宇[b,*], 朱　威[c]

[a]西安交通大学, 人居环境与建筑工程学院, 陕西西安710049

[b]中国科学院地球环境研究所, 黄土第四纪地质国家重点实验室&气溶胶化学与物理重点实验室, 陕西西安710061

[c]香港理工大学, 建设与环境学院, 香港

摘要: 抗生素污染对水生和陆地生态环境系统造成严重的威胁. 在世界各地的水性环境中普遍检测到第二代合成氟喹诺酮类抗生素—诺氟沙星. 因此, 水环境中残留诺氟沙星的去除成为当今研究热点. 在现有去除方法中, 光催化技术因其采用太阳光作为能源、污染物完全矿化及不产生二次污染等优点而被认为是非常有效的方法, 在水处理工业中得到了广泛的关注. 已有研究表明, pH值是影响光催化降解污染物的一个重要因素, 大多数半导体光催化剂的最佳pH被限制在较窄的近中性范围内. 当pH变为酸性或碱性时, 污染物的降解速度显著降低. 我们研究发现, 在太阳光下钨酸铋(SSL/Bi_2WO_6)催化降解诺氟沙星时, 在pH=5.0–10.8表现出较快的去除速率, 其中pH=8.6时效果最佳, 目前优化降解效果多通过酸碱调整初始溶液的pH至最佳值. 进一步研究发现, 即使将反应初始溶液pH值调整到最佳, 随着诺氟沙星的不断降解, 反应溶液的pH值持续降低直至3.0. 溶液不断酸化导致偏离最佳条件, 从而减缓诺氟沙星的降解. 这说明通过简单的酸碱滴定优化溶液初始pH值不能阻止反应过程中溶液的酸化, 也不能解决酸化导致的降效问题. 基于上述问题, 本文提出针对溶液pH值改变对体系效率影响的新方法.

本文以钙钛矿结构的Bi_2WO_6为光催化剂, 诺氟沙星为探针化合物, 详细研究了在不同pH值下SSL/Bi_2WO_6体系催化性能. 为描述SSL/Bi_2WO_6反应的合理性, 首先提出了OH^-富集Bi_2WO_6模型, 并考察了Mg^{2+}和Ca^{2+}两种离子对反应的影响. 在预吸附阶段pH值明显降低, 说明溶液中的羟基离子被吸附到Bi_2WO_6表面. 光催化反应开始后, pH值以较低的速率持续降低, 说明在降解过程中溶液中的羟基离子可能由于低分子有机酸和二氧化碳的形成而逐渐被消耗. 因此, 在Bi_2WO_6表面及其附近维持较高浓度的羟基离子是改善或保持探针快速分解的关键途径. 我们在极碱pH环境中引入NH_4^+缓冲体系, 以持续提供羟基离子生成·OH自由基, 同时可防止溶液酸化, 从而使诺氟沙星的去除率和矿化率在碱性条件下均达到更好的效果. 另一方面, 在酸性pH条件下, 通过加入铁盐(即形成替代的SSL/Fe^{3+}/Bi_2WO_6过程)显著提高了SSL/Bi_2WO_6去除诺氟沙星的效率. 这主要归因于SSL/Fe^{3+}提供的均匀光敏化机制; 同时, Fe^{3+}在SSL/Bi_2WO_6过程中对电子传递起到辅助作用. SSL/Fe^{3+}/Bi_2WO_6工艺可以在较宽的酸性pH(2–4)范围内使用, 且pH=3.0时性能最好. 在SSL/Fe^{3+}/Bi_2WO_6过程中, 诺氟沙星的降解速率随着[Fe3+]的增加而增大, 过剂量时降解趋于平稳.

关键词: 钨酸铋; 扩展pH范围; 诺氟沙星; 光催化; 水

收稿日期: 2018-11-13. 接受日期: 2018-12-13. 出版日期: 2019-05-05.

*通讯联系人. 电话/传真: (029)62336261; 电子信箱: huangyu@ieecas.cn

基金来源: 国家自然科学基金(41877481, 41503102); 中国科学院地球环境研究所黄土第四纪地质国家重点实验室开放课题(SKLLQG1729); 中国博士后科学基金(2018M643669); 中央高校基本科研业务费专项资金(xjj2018249); 中国科学院"百人计划".

本文的电子版全文由Elsevier出版社在ScienceDirect上出版(http://www.sciencedirect.com/science/journal/18722067).